


Critical behavior of active Brownian particles

Jonathan Tammo Siebert, Florian Dittrich, Friederike Schmid, Kurt Binder, Thomas Speck, and Peter Virnau^{*}
Institute for Physics, Johannes Gutenberg University Mainz, 55128 Mainz, Germany

 (Received 7 December 2017; revised manuscript received 28 March 2018; published 18 September 2018)

We study active Brownian particles as a paradigm for a genuine nonequilibrium phase transition requiring steady driving. Access to the critical point in computer simulations is obstructed by the fact that the density is conserved. We propose a method based on arguments from finite-size scaling to determine critical points and successfully test it for the two-dimensional (2D) Ising model. Using this method allows us to accurately determine the critical point of two-dimensional active Brownian particles at $Pe_{cr} = 40(2)$, $\phi_{cr} = 0.597(3)$. Based on this estimate, we study the corresponding critical exponents β , γ/ν , and ν . Our results are incompatible with the 2D-Ising exponents, thus raising the question whether there exists a corresponding nonequilibrium universality class.

DOI: [10.1103/PhysRevE.98.030601](https://doi.org/10.1103/PhysRevE.98.030601)

The notion “active matter” encompasses a wide range of systems and phenomena at the border of physics, chemistry, and biology that share a common trait: they are out of thermal equilibrium due to *local* dissipation stemming from the *directed motion* of its constituents. Examples range from actomyosin [1–3] (actin filaments driven by molecular motors) to swimming bacteria [4,5] to colloidal particles propelled by a multitude of mechanisms [6–14]. The interplay of interactions with this persistent motion leads to a variety of collective dynamic behaviors such as swarming [15], turbulent motion [16], giant number fluctuations [17–19], and clustering [20–25]. In the language of statistical physics, this behavior often can be characterized as “phases” with abrupt changes depending on external parameters such as temperature and density.

Such phase transitions have been investigated intensively, and much has been learned from the study of minimal model systems. The arguably simplest model that shows an order-disorder phase transition ending in a critical point is the Ising model of a lattice of spins interacting with their nearest neighbors. In particular, the understanding of critical points has sparked intensive research that has culminated in the development of tools such as the renormalization group and finite-size scaling in computer simulations that have found application in a wide range of problems. Specifically the system-size dependence of order parameter fluctuations and the crossing of cumulants has proven to be very successful [26–29]. Denoting the order parameter as m , the ratio

$$Q_\ell = \langle m_\ell^2 \rangle^2 / \langle m_\ell^4 \rangle \quad (1)$$

becomes independent of system size ℓ exactly at the critical point. Hence, plotting this quantity for several values of ℓ versus a suitable control parameter allows one to locate the critical point from the intersection with high accuracy.

Universal behavior and scaling invariance are not restricted to passive systems but are also observed in systems driven away from thermal equilibrium. A well-studied paradigm

constitutes the Kardar-Parisi-Zhang equation, originally proposed for the evolution of interfaces [30]. Regarding phase transitions, systems ranging from directed percolation [31], driven diffusive systems [32], to Kuramoto-type coupled oscillator systems [33] have been examined before. However, in the context of active matter, previous studies have focused on nonequilibrium effects on the critical point and the critical exponents of an underlying *equilibrium* phase transition. Examples include two-dimensional and three-dimensional Ising models under shear [34–37] and active versions of the Ising model [38,39]. In the context of active particles, the influence of self-propulsion on the gas-liquid transition in the continuous Asakura-Oosawa model [40] (with alignment interactions) and in a Lennard-Jones fluid [41] (without alignment interactions) have been determined.

While driving a system featuring a passive transition influences its critical behavior, genuine nonequilibrium transitions without a passive counterpart are much less studied. Active Brownian particles (ABPs) have emerged as a minimal model showing such a transition: the coexistence of dilute and dense regions in the absence of cohesive forces [23,42–47]. While the binodal lines away from the critical point have already been determined [23,42,44,48] with good accuracy, the precise position of the critical point remains unknown. It has been estimated in Ref. [49] from an effective equation of state and in Ref. [50] from fitting the binodals. The close resemblance with passive phase separation suggests that density fluctuations of ABPs become scale invariant in the vicinity of the critical point. In the following, we employ extensive computer simulations to shed light on the critical behavior of ABPs and the intriguing possibility of a novel nonequilibrium universality class.

To be specific, we simulate N particles moving in $d = 2$ dimensions in a box with periodic boundary conditions along both dimensions. The coupled equations of motion read

$$\dot{\mathbf{r}}_k = -\nabla_k U + \frac{Pe}{d_{BH}/\sigma} \begin{pmatrix} \cos \varphi_k \\ \sin \varphi_k \end{pmatrix} + \sqrt{2} \mathbf{R}_k \quad (2)$$

with normal distributed Gaussian noise \mathbf{R}_k and potential energy U modeling short-range repulsion with effective hard

^{*}Corresponding author: virnau@uni-mainz.de

disk diameter d_{BH} and unit of length σ . Every particle has an orientation, the evolution of which is described by the angle φ_k undergoing free rotational diffusion with diffusion coefficient D_r . Particles are propelled along this orientation with constant speed which implies a steady dissipation. Throughout, we employ dimensionless quantities with the speed given by the Péclet number $\text{Pe} = (3v_0)/(d_{\text{BH}}D_r)$. Further details can be found in the Supplemental Material [51].

To determine critical points in passive fluids and suspensions, best practice is to conduct numerical simulations in the grand canonical ensemble with the total number of particles fluctuating [52–54]. In driven systems, this option is not (yet) available due to the lack of a rigorous free energy. An alternative strategy to sample density fluctuations is block-density-distribution methods [55–59]. By subdividing a simulation box into smaller subboxes, we allow every subbox to have a fluctuating particle number while the remaining system effectively acts as a particle reservoir. Especially in three-dimensional off-lattice systems this approach has proven to be very successful [29]. Even though it only works for a rather small range of intermediate subbox sizes, it provides accurate results in equilibrium [29] as well as nonequilibrium systems [40]. Nonetheless, there are severe drawbacks especially in two dimensions. For off-lattice systems, e.g., a Lennard-Jones fluid in two dimensions, the method seems to work to some extent, but for the 2D Ising model, it completely fails if the underlying simulation takes place in the canonical ensemble [59]. This failure is demonstrated in Fig. 1(a). The plot shows the cumulant ratio Q_ℓ [Eq. (1)] for the subbox magnetization m as a function of temperature T averaged over independent runs for different subbox lengths ℓ using the original block-magnetization-distribution method [26,27,55]. The curves do not cross over a large temperature range around the critical temperature.

This failure can be traced to the biased measurement of the order parameter distribution in the subboxes, which does not reproduce the grand canonical distribution due to the overexpression of interfaces [59]. To solve this problem, we propose an improved block-distribution method [51]. In a nutshell, we exploit the stability of interfaces in a finite system (even in the vicinity of a critical point) to sample subboxes away from the interface. By simulating an elongated box with aspect ratio 1 : 3, we force the system into a slab geometry [see Fig. 1(c)]. Although, close to the critical point, fluctuations increase such that bubbles or even rifts can appear. Going further into the homogeneous region, the slab eventually dissolves. Four subboxes of size $\ell \times \ell$ are placed in the box; two at the center of mass and two shifted by 3ℓ in the x direction. Aside from avoiding the interfaces, the necessary simulations of systems with different sizes then allow one to also eliminate the second length scale that is introduced by the size of the surrounding simulation box in the original method. Including only the indicated boxes into the calculation of the magnetization, the method is indeed able to predict the critical point of the 2D Ising model with remarkable accuracy. Below the critical point, i.e., in the phase-separated region, the $Q_\ell(T)$ curves are ordered going from large values for large subboxes to small values for small subboxes. At the critical temperature the curves now cross and at even higher temperatures, i.e., in the homogeneous region,

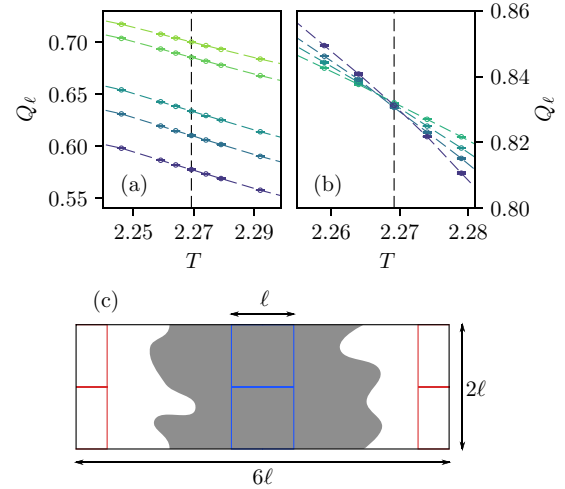


FIG. 1. Critical temperature of the 2D Ising model. (a) Cumulant ratio $Q_\ell(T)$ as a function of temperature T for different subbox sizes $\ell = 5, 6, 10, 12, 15$ (top to bottom) does not cross applying the original block-magnetization-distribution method on an underlying canonical simulation. As discussed in Ref. [59], the cumulants do not intersect due to the presence of interfaces. (b) Using the modified block-magnetization method, $Q_\ell(T)$ curves for different $\ell = 8, 10, 12, 15$ [same color scale as in (a)] now cross very close to the critical temperature $T_c \approx 2.269185$ (indicated by the dashed vertical line) even if the underlying simulation is canonical. (c) Schematic representation of the simulation box used for the cumulant analysis. Simulations are done at medium packing fractions in an elongated box with an edge length ratio of 1:3. This results in a slab geometry where the slab is always aligned with the short axis. Two subboxes are then placed at the center of mass. The other two subboxes are shifted by 3ℓ in the x direction.

they invert their order. This shows that our method indeed allows one to circumvent the main problems of the original block-magnetization-distribution method.

Encouraged by these results, we now return to the active Brownian particles. Analogously to the Ising system, we study simulation boxes with aspect ratio of 1 : 3 and then evaluate subboxes at the center of the dense and the dilute slab [cf. Fig. 1(c)]. In place of the magnetization we employ the subbox density fluctuations $m_\ell = \rho_\ell - \langle \rho_\ell \rangle$ away from the time-averaged density $\langle \rho_\ell \rangle$ and vary the propulsion speed Pe . Here $\rho_\ell = N_\ell/\ell^2$ with N_ℓ the fluctuating number of particles in a subbox with edge length ℓ . The overall packing fraction $\phi = \rho\pi d_{\text{BH}}^2/4 = 0.6$ was chosen to be close to the critical packing fraction as estimated by applying the original subsystem scheme [51]. The resulting curves for $Q_\ell(\text{Pe}) = \langle m_\ell^2 \rangle / \langle m_\ell^4 \rangle$ with values of ℓ between 10 and 17.5 averaged over multiple realization of the system are shown in Fig. 2(b). There is an interval of admissible subsystem sizes outside of which the method fails; a shortcoming that is shared with other block-density-distribution methods [40,59]. To make contact to the physics of hard spheres and previous estimates of the phase diagram [23,42,46], we use the packing fraction ϕ instead of the density. Similarly to the Ising system, the curves show the correct ordering above ($\text{Pe} \geq 42.1$) and below ($\text{Pe} \leq 37.6$) a putative critical point. Between $\text{Pe} = 37.6$ and $\text{Pe} = 42.1$

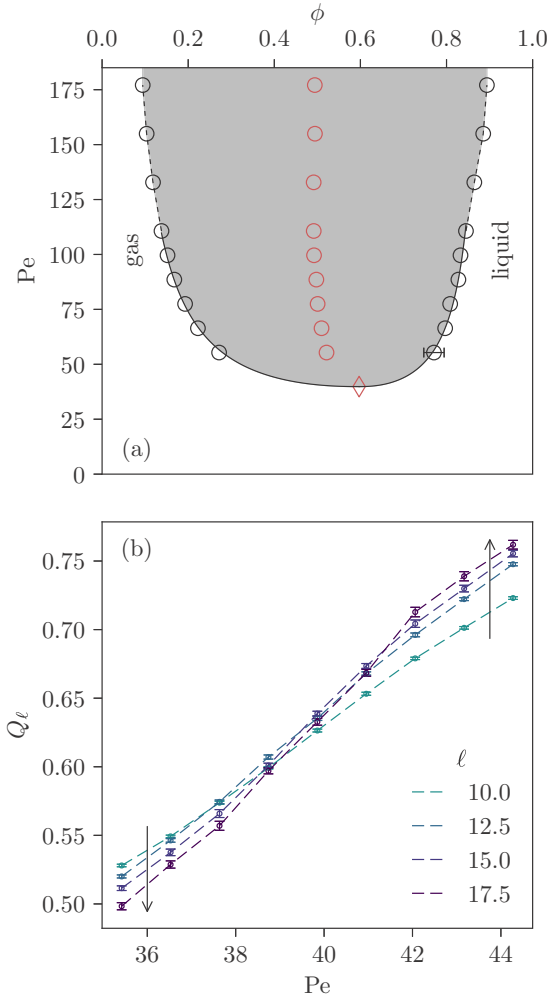


FIG. 2. Critical point of active Brownian particles. (a) Coexisting packing fractions ϕ [23,42] showing our estimate for the critical point as a red diamond. The rectilinear diameter is shown as red circles. For all points without error bars, the statistical uncertainty is smaller than the symbol size. Points far from the critical point ($Pe > 120$) are connected by a dashed line as a guide for the eye. For points close to the critical point, the gas and liquid branches are both fitted with a power law, where the exponent $\beta = 0.45$ is the best estimate arising from our analysis of the critical exponents. (b) Cumulant intersection analysis for ABPs. A crossing of $Q_\ell(Pe)$ [Eq. (1)] for all system sizes ℓ can be seen between $Pe \simeq 38$ and $Pe \simeq 42$, giving an estimate of the critical point of $Pe_{cr} = 40(2)$. Error bars are estimated from independent runs. The dashed lines are again only included as guides to the eye.

the curves cross. This is already a very remarkable result as it supports the notion that scaling behavior as known from equilibrium finite-size scaling is valid also in this nonequilibrium system. Outside this interval, the points corresponding to different edge lengths are clearly separated, whereas within this intermediate interval the points' uncertainties do not allow one to distinguish between them, which in turn indicates that Pe_{cr} lies within this interval. Note that even after eliminating the additional scaling variable of box length over subbox length there are still successive intersections over this region.

Also, even though every point corresponds to between 54 and 174 independent runs that are used to determine the average of $Q_\ell(Pe)$, the resulting uncertainties in Q_ℓ are still notable. Nonetheless, this analysis allows one to estimate the critical point to be at $Pe_{cr} = 40(2)$. To estimate the critical density, we average the mean packing fractions $\langle \phi_\ell \rangle$ over all subbox sizes, all independent runs, and over all Péclet numbers between 37.6 and 42.1. This results in an estimate of $\phi_{cr} = 0.597(3)$. As this is an average over different subbox sizes and Péclet numbers, the uncertainty is given as the standard deviation of the density for all subbox sizes and Péclet numbers each averaged over all respective runs.

Even though our method gives a much more accurate and reliable result, we also checked its consistency with the original block-density-distribution method, which, regardless of its shortcomings, still gives an estimate of the critical point [51]. This estimate is compatible with the results of the modified method excluding interfaces (albeit of course less precise). Furthermore, it is possible to determine a lower bound for the critical speed based on the divergence of the static structure factor, as well as an upper bound by analyzing the cluster size distribution. Both bounds agree well with our current estimate. Altogether, we can conclude that the critical point of ABPs is located at $Pe_{cr} = 40(2)$ and $\phi_{cr} = 0.597(3)$. This point is shown as a red diamond in the phase diagram in Fig. 2(a). Notably, the critical point of ABPs does not lie on the linear extension of the rectilinear diameter, which is shown as red circles. While this is rather uncommon in equilibrium systems, a similar behavior has been found for other nonequilibrium transitions as well [40,41].

We now extract numerical estimates for the critical exponents allowing insight into the critical behavior and the universality class of ABPs. For this purpose, we define the dimensionless distance

$$\tau = \frac{Pe^{-1} - Pe_{cr}^{-1}}{Pe_{cr}^{-1}} \quad (3)$$

to the critical point, generalizing the usual expression by treating the propulsion speed as an inverse temperature. First, we turn to the order parameter exponent β . In the phase-separated region, but still close to the critical point, one expects a power-law increase of the mean order parameter $\langle m \rangle \propto \tau^\beta$ [see Fig. 3(a)]. To account for the uncertainty in the determination of Pe_{cr} , we show three curves corresponding to our best estimate of $Pe_{cr} \simeq 40$ as well as (generous) lower and upper bounds of 37.6 and 42.1, respectively. All three curves show a reasonably linear behavior within the uncertainties of the order parameter. Instead of a fit, as guides we show the slopes corresponding to 2D Ising ($\beta = 1/8$), three-dimensional (3D) Ising ($\beta \approx 0.326$), and mean field (MF) ($\beta = 1/2$). For all reasonable estimates of Pe_{cr} , the slope of the resulting curve is significantly higher than that of the 2D Ising universality behavior.

Both the finite-size behavior of Q_ℓ and the behavior of the order parameter approaching the critical point indicate that usual scaling arguments are applicable, with scale-free density fluctuations at the critical point. This implies the existence of a correlation length ξ that diverges as $\xi \sim \tau^{-\nu}$ with

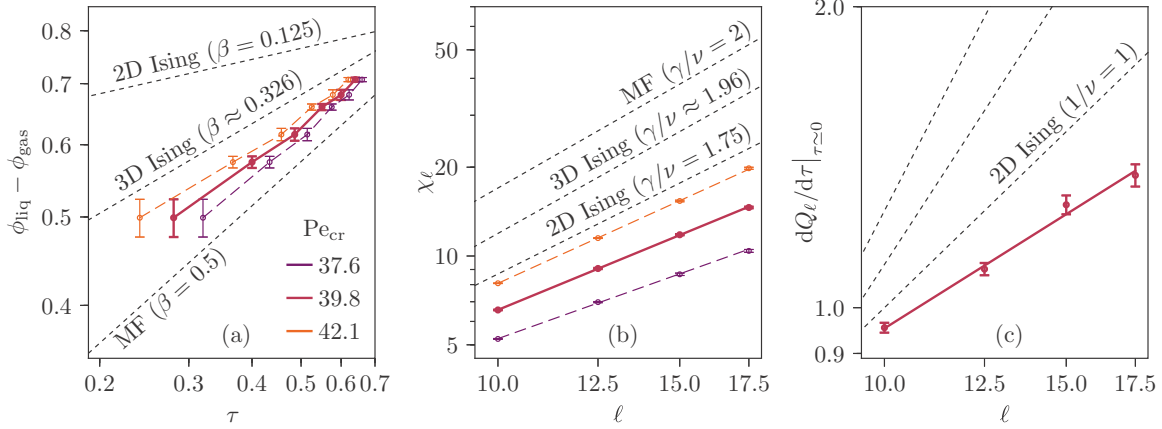


FIG. 3. Determination of critical exponents [thick lines correspond to the estimate of Pe_{cr} , the dashed lines show lower (purple) and upper (orange) bounds]. (a) Log-log plot of the order parameter $\langle m \rangle \propto \phi_{\text{liq}} - \phi_{\text{gas}}$ vs the distance to the critical point τ [Eq. (3)] for different estimates of the critical speed. Connecting lines are shown as guides to the eye. The order parameter exponent β is given by the slope of the curve. Ising and mean-field (MF) slopes are shown as dashed lines for reference. (b) Log-log plot of the particle number fluctuations’ dependence on the subbox size. Their slope corresponds to γ/ν with the susceptibility exponent γ and the correlation length exponent ν . Again, Ising and MF slopes are shown as dashed lines for reference. (c) Log-log plot of Q_ℓ ’s slope against the subbox size. The derivative $dQ_\ell/d\tau|_{\tau=0}$ is determined by fitting a linear function to $Q_\ell(\tau)$ over the full width of the critical region. The slope of the curve in the log-log plot corresponds to $1/\nu$ [51]. 2D-Ising ($\nu = 1$), 3D-Ising ($\nu \simeq 0.63$), and MF ($\nu = 1/2$) universality are shown for reference as dashed lines in increasing order of steepness.

exponent ν . Assuming that the susceptibility

$$\chi_\ell = \frac{\langle (N_\ell - \langle N_\ell \rangle)^2 \rangle}{\langle N_\ell \rangle} \quad (4)$$

diverges as $\chi_\infty \sim \tau^{-\nu}$ in the infinite size limit, one derives the relation $\chi_\ell = \chi_0(\ell/\xi)\xi^{\nu/\nu} = \ell^{\nu/\nu}\tilde{\chi}(x)$ with scaling function $\tilde{\chi}(x)$ replacing τ by ξ and assuming a prefactor χ_0 that depends on system size only through the ratio $x = \ell/\xi$. Since ξ is bound by the smaller dimension of the full box 2ℓ and the quotient of that length and the subbox height is fixed, close to the critical point the scaling function saturates to a constant value and we can extract the ratio of γ/ν from the slope of the calculated χ_ℓ plotted against ℓ in Fig. 3(b). We see that the resulting slope is again smaller than that expected for 2D Ising ($\gamma/\nu = 1.75$), and even farther from 3D Ising ($\gamma/\nu \approx 1.96$) or MF ($\gamma/\nu = 2$).

Finally, we turn to the dependence of Q_ℓ ’s derivative with respect to the distance from the critical point around criticality: $dQ_\ell/d\tau|_{\tau=0}$. It is expected to have a power-law dependence on the system size ℓ with exponent $1/\nu$ [51]. To estimate the derivative, we fit $Q_\ell(\tau)$ in the region where we estimated the critical point [$Pe = 40(2)$] with a linear function. Its dependence on the system size is shown in Fig. 3(c). The slope of this curve is significantly lower than that expected for 2D Ising ($1/\nu = 1$), indicating that $\nu > 1$, which agrees with the much stronger fluctuations observed for ABPs compared to passive phase coexistence. As demonstrated in the Supplemental Material [51], less than a decade in ℓ is amply sufficient to deduce the exponents with reasonable precision (a few percent), as is well known [60]. Using rough estimates for the critical exponents ($\beta \simeq 0.45$, $\nu \simeq 1.5$, and $\gamma \simeq 2.2$), a tentative check of the scaling relation $\gamma + 2\beta = 2\nu$ shows that it is approximately satisfied. While the derivations of scaling relations for an equilibrium system are typically based on a well-defined free energy scaling ansatz, our analysis is based on an analogy to equilibrium phase transitions.

The fact that the scaling relation seems to hold (which, given the numerical uncertainties) is interesting in itself.

Within a mean-field treatment of Eq. (2), the qualitative phase behavior of ABPs is indeed recovered with a critical point characterized by the expected mean-field exponents [50]. The relevant nonlinearity $\sim \rho^4$ is that of the Ising class for short-range interactions. Hence, in the presence of additive noise one would expect that the critical point also falls into the Ising universality class. Somewhat surprisingly (given the strong resemblance with ordinary phase separation), our numerical results indicate that this might not be the case. Extracting critical exponents from numerical data crucially depends on the precise determination of the critical point. An exact determination, which would allow a definite answer to the question of the existence of an “active matter” universality class, is still precluded by the statistical uncertainties in the determination of the critical point. Nevertheless, our best estimate $Pe_{\text{cr}} \simeq 40(2)$ for the critical speed implies that all exponents do not agree with the corresponding 2D Ising values (cf. Fig. 3 in Ref. [61]).

To conclude, we were able to determine the critical point of ABPs to be at $Pe_{\text{cr}} = 40(2)$ and $\phi_{\text{cr}} = 0.597(3)$. Moreover, we have provided numerical evidence that the universality class might not agree with Ising 2D universality despite the strong qualitative agreement with passive liquid-gas phase separation. This is somewhat unexpected and we hope that these results will stimulate further research into the theoretical underpinning of scale invariance in active matter and genuine nonequilibrium phase transitions.

J.T.S., T.S., and P.V. gratefully acknowledge financial support by the Deutsche Forschungsgemeinschaft within priority program SPP 1726 (Grants No. SP1382/3-2 and No. VI 237/5-2). ZDV Mainz is acknowledged for computing time on the MOGON supercomputers.

- [1] G. H. Koenderink, Z. Dogic, F. Nakamura, P. M. Bendix, F. C. MacKintosh, J. H. Hartwig, T. P. Stossel, and D. A. Weitz, *Proc. Natl. Acad. Sci. USA* **106**, 15192 (2009).
- [2] V. Schaller, C. Weber, C. Semmrich, E. Frey, and A. R. Bausch, *Nature (London)* **467**, 73 (2010).
- [3] T. Sanchez, D. T. N. Chen, S. J. DeCamp, M. Heymann, and Z. Dogic, *Nature (London)* **491**, 431 (2012).
- [4] H. P. Zhang, A. Be'er, E.-L. Florin, and H. L. Swinney, *Proc. Natl. Acad. Sci. USA* **107**, 13626 (2010).
- [5] H. H. Wensink, J. Dunkel, S. Heidenreich, K. Drescher, R. E. Goldstein, H. Lowen, and J. M. Yeomans, *Proc. Natl. Acad. Sci. USA* **109**, 14308 (2012).
- [6] W. F. Paxton, P. T. Baker, T. R. Kline, Y. Wang, T. E. Mallouk, and A. Sen, *J. Am. Chem. Soc.* **128**, 14881 (2006).
- [7] Y. Hong, N. M. K. Blackman, N. D. Kopp, A. Sen, and D. Velegol, *Phys. Rev. Lett.* **99**, 178103 (2007).
- [8] J. Palacci, C. Cottin-Bizonne, C. Ybert, and L. Bocquet, *Phys. Rev. Lett.* **105**, 088304 (2010).
- [9] H.-R. Jiang, N. Yoshinaga, and M. Sano, *Phys. Rev. Lett.* **105**, 268302 (2010).
- [10] I. Buttinoni, J. Bialké, F. Kümmel, H. Löwen, C. Bechinger, and T. Speck, *Phys. Rev. Lett.* **110**, 238301 (2013).
- [11] R. Dreyfus, J. Baudry, M. L. Roper, M. Fermigier, H. A. Stone, and J. Bibette, *Nature (London)* **437**, 862 (2005).
- [12] K. Peddireddy, P. Kumar, S. Thutupalli, S. Herminghaus, and C. Bahr, *Langmuir* **28**, 12426 (2012).
- [13] S. Herminghaus, C. C. Maass, C. Krüger, S. Thutupalli, L. Goehring, and C. Bahr, *Soft Matter* **10**, 7008 (2014).
- [14] W. Wang, L. A. Castro, M. Hoyos, and T. E. Mallouk, *ACS Nano* **6**, 6122 (2012).
- [15] H. H. Wensink and H. Löwen, *J. Phys.: Condens. Matter* **24**, 464130 (2012).
- [16] C. Dombrowski, L. Cisneros, S. Chatkaew, R. E. Goldstein, and J. O. Kessler, *Phys. Rev. Lett.* **93**, 098103 (2004).
- [17] S. Ramaswamy, R. A. Simha, and J. Toner, *Europhys. Lett.* **62**, 196 (2003).
- [18] S. Ramaswamy, *Annu. Rev. Condens. Matter Phys.* **1**, 323 (2010).
- [19] V. Narayan, S. Ramaswamy, and N. Menon, *Science* **317**, 105 (2007).
- [20] J. Bialké, T. Speck, and H. Löwen, *Phys. Rev. Lett.* **108**, 168301 (2012).
- [21] S. K. Das, S. A. Egorov, B. Trefz, P. Virnau, and K. Binder, *Phys. Rev. Lett.* **112**, 198301 (2014).
- [22] B. Trefz, S. K. Das, S. A. Egorov, P. Virnau, and K. Binder, *J. Chem. Phys.* **144**, 144902 (2016).
- [23] J. T. Siebert, J. Letz, T. Speck, and P. Virnau, *Soft Matter* **13**, 1020 (2017).
- [24] B. Ezhilan, R. Alonso-Matilla, and D. Saintillan, *J. Fluid Mech.* **781**, R4 (2015).
- [25] R. Wittkowski, A. Tiribocchi, J. Stenhammar, R. J. Allen, D. Marenduzzo, and M. E. Cates, *Nat. Commun.* **5**, 4351 (2014).
- [26] E. Luijten, *Phys. Rev. E* **60**, 7558 (1999).
- [27] E. Luijten, M. E. Fisher, and A. Z. Panagiotopoulos, *Phys. Rev. Lett.* **88**, 185701 (2002).
- [28] M. Camprostrini, M. Hasenbusch, A. Pelissetto, P. Rossi, and E. Vicari, *Phys. Rev. B* **63**, 214503 (2001).
- [29] H. Watanabe, N. Ito, and C.-K. Hu, *J. Chem. Phys.* **136**, 204102 (2012).
- [30] M. Kardar, G. Parisi, and Y.-C. Zhang, *Phys. Rev. Lett.* **56**, 889 (1986).
- [31] H. Hinrichsen, *Adv. Phys.* **49**, 815 (2000).
- [32] B. Derrida, *J. Stat. Mech.: Theor. Exp.* (2007) P07023.
- [33] F. Dörfler and F. Bullo, *Automatica* **50**, 1539 (2014).
- [34] D. Winter, P. Virnau, J. Horbach, and K. Binder, *Europhys. Lett.* **91**, 60002 (2010).
- [35] A. Hucht, *Phys. Rev. E* **80**, 061138 (2009).
- [36] S. Angst, A. Hucht, and D. E. Wolf, *Phys. Rev. E* **85**, 051120 (2012).
- [37] A. Hucht and S. Angst, *Europhys. Lett.* **100**, 20003 (2012).
- [38] A. P. Solon and J. Tailleur, *Phys. Rev. E* **92**, 042119 (2015).
- [39] A. Attanasi, A. Cavagna, L. Del Castello, I. Giardina, T. S. Grigera, A. Jelić, S. Melillo, L. Parisi, O. Pohl, E. Shen *et al.*, *Nat. Phys.* **10**, 691 (2014).
- [40] B. Trefz, J. T. Siebert, T. Speck, K. Binder, and P. Virnau, *J. Chem. Phys.* **146**, 074901 (2017).
- [41] V. Prymidis, S. Paliwal, M. Dijkstra, and L. Filion, *J. Chem. Phys.* **145**, 124904 (2016).
- [42] J. Bialké, J. T. Siebert, H. Löwen, and T. Speck, *Phys. Rev. Lett.* **115**, 098301 (2015).
- [43] Y. Fily and M. C. Marchetti, *Phys. Rev. Lett.* **108**, 235702 (2012).
- [44] G. S. Redner, M. F. Hagan, and A. Baskaran, *Phys. Rev. Lett.* **110**, 055701 (2013).
- [45] A. P. Solon, J. Stenhammar, R. Wittkowski, M. Kardar, Y. Kafri, M. E. Cates, and J. Tailleur, *Phys. Rev. Lett.* **114**, 198301 (2015).
- [46] J. Stenhammar, D. Marenduzzo, R. J. Allen, and M. E. Cates, *Soft Matter* **10**, 1489 (2014).
- [47] A. Wysocki, R. G. Winkler, and G. Gompper, *Europhys. Lett.* **105**, 48004 (2014).
- [48] D. Levis, J. Codina, and I. Pagonabarraga, *Soft Matter* **13**, 8113 (2017).
- [49] S. C. Takatori and J. F. Brady, *Phys. Rev. E* **91**, 032117 (2015).
- [50] T. Speck, A. M. Menzel, J. Bialké, and H. Löwen, *J. Chem. Phys.* **142**, 224109 (2015).
- [51] See Supplemental Material at <http://link.aps.org/supplemental/10.1103/PhysRevE.98.030601> for a detailed description of the model and the improved block-distribution method, a qualitative justification for the crossing of cumulants, the results of the original subsystem method, and an analysis of the static structure factor (citing Refs. [62–74]).
- [52] A. D. Bruce and N. B. Wilding, *Phys. Rev. Lett.* **68**, 193 (1992).
- [53] N. B. Wilding, *Phys. Rev. E* **52**, 602 (1995).
- [54] N. B. Wilding, *J. Phys.: Condens. Matter* **9**, 585 (1997).
- [55] K. Binder, *Z. Phys. B Condens. Matter* **43**, 119 (1981).
- [56] K. Binder, *Ferroelectrics* **73**, 43 (1987).
- [57] M. Rovere, D. W. Hermann, and K. Binder, *Europhys. Lett.* **6**, 585 (1988).
- [58] M. Rovere, D. W. Heermann, and K. Binder, *J. Phys.: Condens. Matter* **2**, 7009 (1990).
- [59] M. Rovere, P. Nielaba, and K. Binder, *Z. Phys. B: Condens. Matter* **90**, 215 (1993).
- [60] D. P. Landau and K. Binder, *A Guide to Monte Carlo Simulations in Statistical Physics* (Cambridge University Press, Cambridge, UK, 2014).
- [61] Furthermore, we can exclude that our data can be interpreted as a crossover between nontrivial criticality and mean-field behavior. In equilibrium systems, such a crossover is seen in

- systems with medium range of the interactions and occurs then, according to the Ginzburg criterion, rather close to the critical point. All our data are not very close to the critical point, and the interactions have very short range, so there is no physical basis for such an interpretation. Moreover, the slopes in Figs. 3(b) and 3(c) are not in between Ising and MF values.
- [62] J. D. Weeks, D. Chandler, and H. C. Andersen, *J. Chem. Phys.* **54**, 5237 (1971).
- [63] J. A. Barker and D. Henderson, *J. Chem. Phys.* **47**, 4714 (1967).
- [64] P. Kloeden and E. Platen, *Numerical Solution of Stochastic Differential Equations*, 3rd ed. (Springer, Berlin/Heidelberg, 1999), pp. 505–506.
- [65] L. Bai and D. Breen, *J. Graph GPU Game Tools* **13**, 53 (2008).
- [66] D. Abraham, in *Phase Transitions and Critical Phenomena*, edited by J. L. C. Domb (Academic, London, 1986), Vol. 10, Chap. 1.
- [67] K. Binder, in *Cohesion and Structure*, edited by F. de Boer and D. Pettifor (North-Holland, Amsterdam, 1995), Vol. 4, Chap. 3, pp. 121–283.
- [68] L. Landau and E. Lifshitz, *Statistical Physics: Course of Theoretical Physics* (translated from Russian by E. Peierls and R. F. Peierls) (Pergamon, New York, 1958).
- [69] F. Román, J. White, and S. Velasco, *J. Chem. Phys.* **106**, 4196 (1997).
- [70] F. Román, J. White, and S. Velasco, *Europhys. Lett.* **42**, 371 (1998).
- [71] S. Sengupta, P. Nielaba, M. Rao, and K. Binder, *Phys. Rev. E* **61**, 1072 (2000).
- [72] Y. C. Kim, M. E. Fisher, and E. Luijten, *Phys. Rev. Lett.* **91**, 065701 (2003).
- [73] Y. C. Kim and M. E. Fisher, *Phys. Rev. E* **68**, 041506 (2003).
- [74] M. E. Fisher, *J. Math. Phys.* **5**, 944 (1964).